Improved Experimental Limits on the Production of Magnetic Monopoles

G. R. Kalbfleisch,* K. A. Milton, M. G. Strauss, L. Gamberg, E. H. Smith,† and W. Luo

Department of Physics and Astronomy, University of Oklahoma, Norman, Oklahoma 73019

(May 2, 2000)

We present new limits on low mass accelerator-produced point-like Dirac magnetic monopoles trapped and bound in matter surrounding the DØ collision region of the Tevatron at Fermilab (experiment E-882). In the context of a Drell-Yan mechanism, we obtain cross section limits for the production of monopoles with magnetic charge values of 1, 2, 3, and 6 times the minimum Dirac charge of the order of picobarns, some hundred times smaller than found in similar previous Fermilab searches. Mass limits inferred from these cross section limits are presented.

14.80.Hv,13.85.Rm,07.55.-w

The existence of magnetic monopoles of charge g explains the quantization of electric charge e as $eg = n\hbar c/2$, $n = \pm 1, \pm 2, \ldots$ [1], results in the dual-symmetrization of Maxwell's equations [2], and is not forbidden by any known principles of physics. The minimum values of the quantization number are $n = 1$ according to Dirac and $n = 2$ according to Schwinger [1]. For e being the charge on the electron, these values are $n = 3$ and $n = 6$, respectively, if quantization with the quark electric charges is allowed. Previous searches for trapped and bound magnetic monopoles in samples from various accelerators [3,4], in meteorites [5], and lunar soil [6] have been made. Since the Tevatron proton-antiproton ($p\bar{p}$) collider has extended its integrated luminosity by a factor of some ten thousand over the last search of Bertani et al. [4], we have taken samples exposed in the DØ experiment and performed a search that improves these limits. We use the induction method of Alvarez et al. [7] to measure the magnetic charge content of macroscopic Al and Be samples. Indirect searches [8] are able to present limits beyond those energetically allowed in direct searches, but represent an entirely different set of assumptions as to their observation, and are not further discussed in this letter. We also do not discuss very massive GUT monopoles, such as those searched for in cosmic rays [9].

This extension of limits is experimentally driven. Theoretical motivation, beyond the general principles given above, derives from the possibility that magnetic monopoles generated during spontaneous symme-try breaking at the electroweak scale might give rise to monopoles of mass ~ 2.5 to ~ 15 TeV [10]. The search here can only raise the previous limits of ~ 0.1 TeV to ~ 0.4 TeV. At the Large Hadron Collider one could approach 2 TeV with the same techniques.

A large warm bore cryogenic detector, similar to that of Longo et al. [5], was constructed and operated at the University of Oklahoma. The active elements of the detector are two 19 cm diameter superconducting loops each connected to a DC SQUID (Superconducting QUantum Interference Device) [11]. The Meisner effect prevents a change in the net flux through the loops, resulting in a change, or "step," in current flowing in the loops whenever a magnetic charge passes through them. Samples of a size less than 7.5 cm in diameter by 7.5 cm in length are repeatedly passed through the 10 cm diameter warm bore centered on and perpendicular to the loops, traveling some 108 cm about the position of the superconducting loops. In a central 64 cm region this allows for the magnetic effects of induced and permanent dipole moments in the sample to start and return to zero on each up and each down traversal of the sample. High frequency noise is filtered out, while random and $1/f$ noise contributions are averaged out over 20 pairs of up/down passes. Each up or down traversal takes some 25 seconds. A net data rate of 10 Hz is recorded for each of the two SQUIDs; recorded as well are the readings from an accelerometer, the vertical position from an optical encoder, the number of increments taken by the stepper motor, and the time.

The SQUIDs are tuned and their transfer functions measured periodically according to the manufacturer's specifications in order to keep them operating with constant sensitivity. The absolute calibration of an expected signal from a Dirac monopole was made using a "pseudopole." A long thin magnetic solenoid (1.5 cm diameter by 100 cm length with 4710 turns per meter) carrying a calibrated small current gives a calculable pseudopole at either end. This pseudopole can either be passed through the warm bore of the detector in a way similar to the samples, or it can be placed in a given position with one end fully extended through the SQUID loops and the solenoid current repeatedly switched on and off. Both methods were used and a value of 2.40 ± 0.04 mV/minimum Dirac charge was obtained. The internal random and systematic local noise contributions were typically 0.2 mV, although the external systematic error of ~ 0.7 mV dominates.

---

*Electronic mail: `grk@mail.nhn.ou.edu`
†Present address: Lockheed Martin, Palo Alto, CA 94304

The shape of the pseudopole curve is compared to that of a theoretical calculation in Fig. 1a and the response to a point magnetic dipole is compared to a narrow one from the data. Fig. 1b shows the step from a 5.5mV (i.e., 2.3 Dirac poles) signal from a run of a pseudopole embedded in an Al sample. The movement of conducting samples through the small residual magnetic field gradient in the warm bore also gives rise to an induced dipole, which cancels out over an up/down pair.
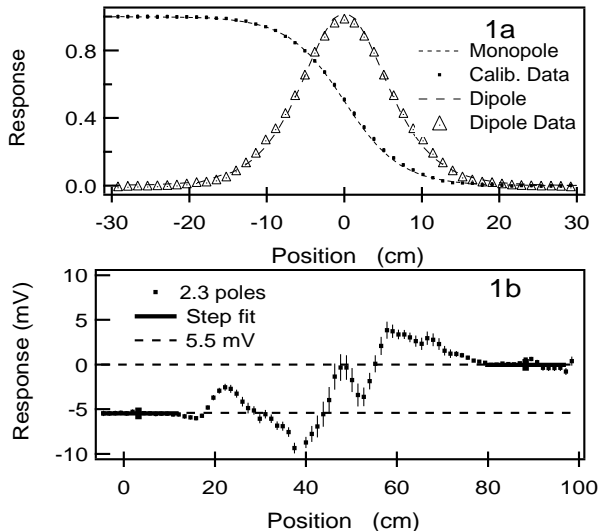

FIG. 1. "Pseudopole" curves. a) Comparison of theoretical monopole response to an experimental calibration and of a simple point dipole of one sample with that calculated from the theoretical response curve. b) The observed "step" for a pseudopole current, corresponding to 2.3 minimum Dirac poles, embedded in an Al sample.

There are two kinds of samples, beryllium and aluminum. A 46 cm section of the 5 cm diameter DØ Be beam pipe, centered on the collision region, covering nearly the full solid angle, was cut into six 7.6 cm pieces. Two extension cylinders of Al, each of 150 cm diameter by 46 cm length and of 1.26 cm thickness, also were cut into pieces of 7 cm by 7.6 cm or of 6 cm by 7.6 cm, and bundled four pieces to a "sample." The effective solid angle acceptance [12] subtended by both extension cylinders was 0.12 of 4π, around a cosine of the laboratory polar angle of -0.82 or 0.82. There were a total of 222 Al samples. Both the Be and Al samples were measured using the aforementioned traversal scheme. Since a nylon string, which could be magnetically contaminated, pulled the samples through the warm bore, we also ran background runs between every two samples.

The data analysis proceeded as follows. The time sequences of the SQUIDs' outputs were examined interactively, and bad sections deleted pairwise (up/down); typically 17–18 pairs of traversals remained. A pedestal value (the SQUID output near the top end of each traversal) was subtracted from every voltage value along that

up (or down) traversal. The values for each of some 90 small ranges of vertical positions were averaged, removing most of the random drift of the SQUIDs. The two SQUIDs' data were averaged, shifting one relative to the other by 10.1 cm in position in order to superimpose their dipole responses. The background samples were analyzed similarly and local groups of background runs were averaged. These backgrounds were subtracted from the samples' spectra. A horizontal line was fit to two regions, one at the lower position and one at the upper, as seen earlier in Fig. 1b; the difference in the values of these two flat fits gives the step for that sample. Examples of sample spectra are shown in Fig. 2a and 2b. The steps from the various samples are histogramed in Fig. 3. The background subtraction ensures that the distribution of steps centers on zero, since the small effect of the magnetized string holding the sample has been removed.
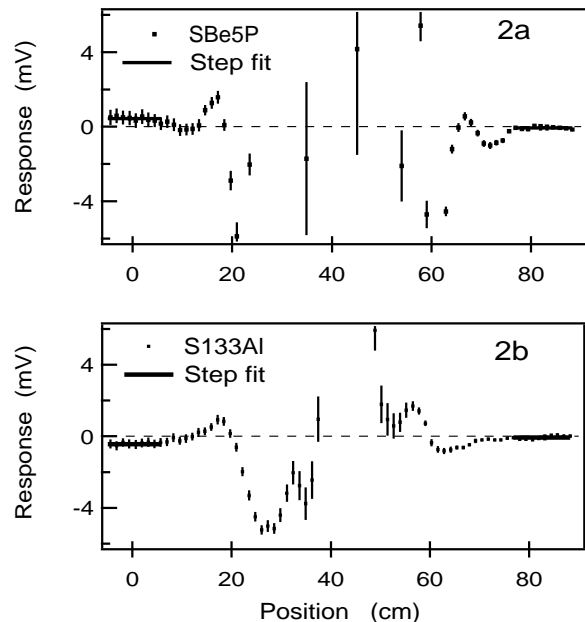

FIG. 2. Sample spectra. a) Beryllium sample "SBe5P," and b) aluminum sample "S133Al." The observed steps are -0.8 mV in a) and $+0.4$ mV in b). The dipole signals are off scale in the middle regions of the plot in this vertically expanded view.

The distribution of steps for the data has a mean of 0.16 mV and an rms spread (sigma) of 0.73 mV, as shown in Fig. 3. One sided 90% confidence limits for monopole charges of $n = 1$ or -1 can be obtained by considering the number of samples that are within 1.28 sigma of the $n = \pm 1$ positions, corresponding to samples outside of the central region of ± 1.47 mV around zero. We find 8 samples outside this central region, where 10.4 were to be expected from the Gaussian error. According to Feldman and Cousins [13], the 90% confidence upper limit is 4.2 signal events for 8 events observed when 10 were expected. In order to be sure that none of the 8 outlying

samples were monopole candidates, we remeasured them along with a few control samples; all eight remeasured samples fell within ± 1.47 mV of $n = 0$.

No samples are within 1.28 sigma of the $|n| \geq 2$ positions, the closest being 3.08 sigma away from $n = -2$. The 90% confidence upper limit is 2.4 signal events for zero events observed and zero expected. The upper limit numbers 4.2 and 2.4 are used to derive cross section upper limits for $|n| = 1$ and $|n| \geq 2$, respectively.
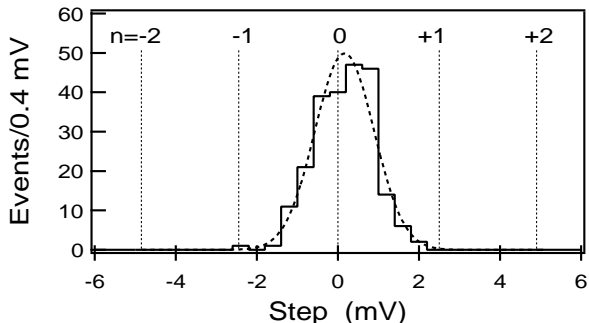

FIG. 3. Histogram of steps. Vertical lines (dashed) define the expected positions of signals for various n. The Gaussian curve (dashed) corresponds to 228 measurements having an average value of 0.16 mV and an rms sigma of 0.73 mV.

The acceptance of the experiment to the stopping and trapping of monopoles must be estimated. It is a function of ranging out of monopoles due to the energy loss in bulk matter and the distribution in energy of the produced monopoles. It is assumed that ranged out and stopped monopoles bind to the magnetic dipole moments of the appropriate nuclei, ^{9}Be or ^{27}Al [14]. The production is assumed to derive from a Drell-Yan process: quark-antiquark annihilation to monopole-antimonopole pair via an intermediate high mass virtual photon. The shape of the energy distribution follows from a dimensional argument that is basic to Drell-Yan: $M^3 d\sigma/dM$ is dimensionless, where M is the invariant mass of the pair of monopoles. This $p\bar{p}$ cross section must include a threshold phase space factor and the velocity dependence of the monopole interaction. The threshold factor is β, the velocity of the monopole in the CM system. We take the interaction factor to be β^2, since the Lorentz force for magnetic charges g is $\mathbf{F} = g(\mathbf{H} - \mathbf{v} \times \mathbf{D})$. Thus the energy shape of $d\sigma/dM$ is $(\beta/M)^3$, convoluted with the momentum distributions of the quarks in the colliding proton and antiproton. In the absence of a theory of monopole cross sections, we are led to make these model assumptions. Fig. 4a shows the shape for the cases $\beta = 1$ and $\beta = v/c$. The acceptance is the area of this distribution between two M limits divided by the area of the total distribution. The two M limits are $M_{\text{low}} = 2m + 2T_{\text{low}}$ and $M_{\text{high}} = 2m + 2T_{\text{high}}$, where m is the mass of each produced monopole and the T's are the kinetic energies of monopoles which are either just entering or just ready to

exit the sample. If the energy is too low or too high, the monopole will not be absorbed by that part of the detector. The energy loss functions as summarized by Ahlen [15] were parameterized as to range, monopole mass, angle, and sample. The estimated acceptances given in Table I vary slowly in the mass regions of interest.

Using the total luminosity delivered to DØ, 172 ± 8 pb^{-1} [16], the number limit of monopoles, the acceptance, and the solid angle coverage given above, we obtain the $p\bar{p}$ cross section limits shown in Table I. These limits are more than 100 times smaller than the best prior Tevatron limit of Bertani et al. [4] of 200 pb.
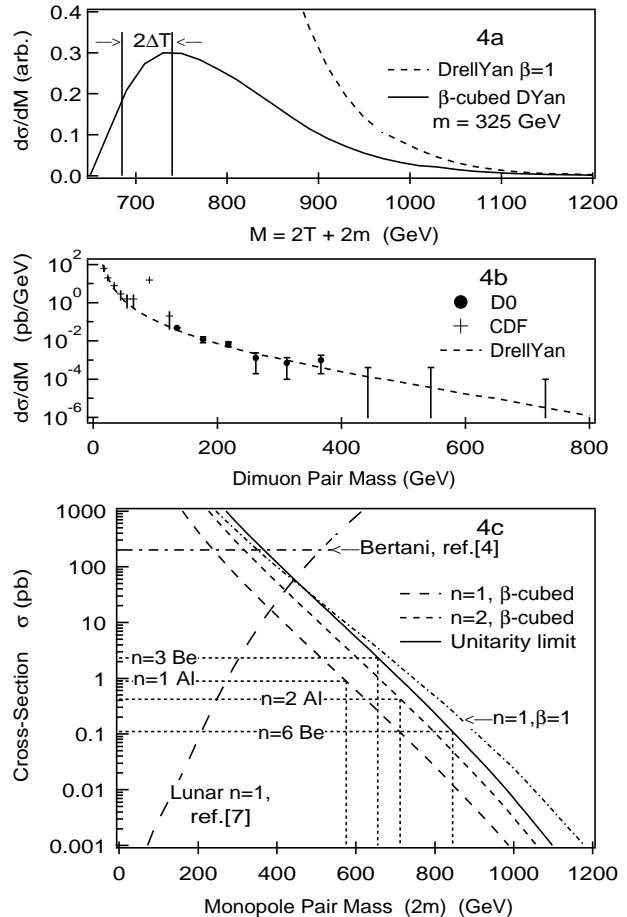

FIG. 4. Cross-section plots. a) $d\sigma/dM$ for Drell-Yan production. The solid curve, cut between the two kinetic energy (T) limits, yields the acceptance for stopping and trapping $n = 1$ monopoles in the aluminum extension cylinder. The dashed curve gives that for dimuons. b) The differential dimuon cross section is normalized to the DØ [18] and CDF [17] dimuon data. c) The $d\sigma/dM$ curve of b) is multiplied by β^3, integrated and renormalized by a factor of $n^2(137/2)^2$ to give the cross section curves versus pair mass $(2m)$ as shown. For the lunar samples, the ordinate is the proton-nucleon cross section. The $n = 1$, $\beta = 1$ curve is shown for comparison because the β^3 correction was not included in previously published limits.

One can further interpret these limits as mass limits

using the scaled Drell-Yan cross sections. Here the cross section is taken to be $n^2(137/2)^2$ larger than the Drell-Yan muon pair cross section, modified by β^3, for $p\bar{p}$ interactions measured by CDF [17] and by DØ [18]. For such large cross sections a unitarity limit appears at an equivalent $n^2 \sim 9$ [19]. We thus use the $n = 1$ or 2 scalings for the cases $n = 1$ or 2, and the unitarity limit for higher n values in converting cross section limits into mass limits. We offer this procedure, as well as that for determining the cross sections, as canonical. We realize that future theoretical work may change this interpretation of the data. The normalization of the Drell-Yan muon pair calculation (using the CTEQ5m parton distribution functions [20]) to the CDF and DØ data are shown in Fig. 4b. The result of the integration of $d\sigma/dM$ to a total cross section for monopoles is shown in Fig. 4c, along with the upper limits for the data of Table I. The Bertani et al. [4] and the lunar rock sample limits of Ross et al. [6] are also shown. The corresponding interpreted lower mass limits are given in Table I. These limits are some 3 times larger than those of prior searches for accelerator-produced monopoles trapped in matter.

ACKNOWLEDGEMENTS

[1] P. A. M. Dirac, Proc. R. Soc. (London) **A133**, 60 (1931); J. Schwinger, Phys. Rev. D **12**, 3105 (1975), and earlier references therein.

[2] For example, J. Schwinger, L. L. DeRaad, Jr., K. A. Milton, and W.-y. Tsai, *Classical Electrodynamics* (Perseus, Reading, MA, 1998).

[3] For example, P. H. Eberhard et al., Phys. Rev. D **11**, 3099 (1975); D. L. Burke et al., Phys. Lett. **60B**, 113 (1975); G. Giacomelli et al., Nuovo Cimento **28A**, 21 (1975); R. A. Carrigan, B. P. Strauss and G. Giacomelli, Phys. Rev. D **17**, 1754 (1978); B. Aubert et al., Phys. Lett. **120B**, 465 (1983); D. Freyberger et al., Phys. Rev. D **29**, 1524 (1984); K. Kinoshita et al., Phys. Rev. Lett. **60**, 1610 (1988) and Phys. Lett. **228B**, 543 (1989); J. Pinfold et al., Phys. Lett. **316B**, 407 (1993).

[4] M. Bertani et al., Eur. Phys. Lett. **12**, 613 (1990); P. B. Price, R. Guoxiao, and K. Kinoshita, Phys. Rev. Lett. **59**, 2523 (1987); P. B. Price, J. Guiri, and K. Kinoshita, Phys. Rev. Lett. **65**, 149 (1990).

[5] H. Jeon and M. J. Longo, Phys. Rev. Lett. **75**, 1443 (1995).

[6] R. R. Ross et al., Phys. Rev. D **8**, 698 (1973).

[7] P. H. Eberhard et al., Phys. Rev. D **4**, 3260 (1971) and L. W. Alvarez, LRL Physics Note-470, 1963 (unpublished).

[8] B. Abbott et al., Phys. Rev. Lett. **81**, 524 (1998).

[9] D. F. Bartlett et al., Phys. Rev. D **24**, 612 (1981); D. E. Groom, Phys. Rep. **140**, 323 (1986); S. Ahlen et al., Phys. Rev. Lett. **72**, 608 (1994); M. Ambrosio et al., Phys. Lett. **406B**, 249 (1997).

[10] J. Preskill, Ann. Rev. Nucl. Sci. **34**, 461 (1984); T. W. Kirkman and C. K. Zachos, Phys. Rev. D **24**, 999 (1981).

[11] Quantum Design, 11578 Sorrento Valley Road, San Diego, CA 92121.

[12] We take into account the longitudinal momentum of the quark-antiquark pair, and assume the production is isotropic in the monopole-pair center of mass frame.

[13] G. J. Feldman and R. D. Cousins, Phys. Rev. D **57**, 3873 (1998), Table IV and V.

[14] For nuclei with spin greater than 1/2 binding should occur when the nuclear gyromagnetic ratio is sufficiently large, so ^{27}Al should bind; on the other hand, treating ^{9}Be as an elementary particle does not allow binding, but we would expect that nuclear structure rearrangement would permit binding. See L. Gamberg, G. R. Kalbfleisch, and K. A. Milton, OKHEP-99-04, hep-ph/9906526, to be published in Kurt Haller's *Festschrift*.

[15] S. P. Ahlen, "Monopole Energy Loss and Detector Excitation Mechanisms," in *Magnetic Monopoles*, ed. R. A. Carrigan and W. P. Trower (Plenum Press, New York, 1982), p. 259.

[16] M. Tartaglia, private communication.

[17] F. Abe et al., Phys. Rev. D **49**, R1 (1994), using an estimated rapidity width of 10 ± 0.5.

[18] B. Abbott et al., Phys. Rev. Lett. **82**, 4769 (1999).

[19] We equate the elementary quark-antiquark reaction cross section to $(2J + 1)\pi/s$ for $J \sim 1$.

[20] H. L. Lai et al., Eur. Phys. J. C **12**, 375 (2000). We note that other PDFs, MRST [A. D. Martin et al., Eur. Phys. J. C **4**, 463 (1998)] and GRV [M. Glück, E. Reya, and A. Vogt, Eur. Phys. J. C **5**, 461 (1998)] agree within a few percent with CTEQ.

Magnetic Charge	$|n| = 1$	$|n| = 2$	$|n| = 3$	$|n| = 6$
Sample	Al	Al	Be	Be
$\Delta\Omega/4\pi$ acceptance	0.12	0.12	0.95	0.95
Mass Acceptance	0.23	0.28	0.0065	0.13
Number of Poles	< 4.2	< 2.4	< 2.4	< 2.4
Upper limit on cross section	0.88 pb	0.42 pb	2.3 pb	0.11 pb
Monopole Mass Limit	> 285 GeV	> 355 GeV	> 325 GeV	> 420 GeV

TABLE I. Acceptances, upper cross section limits, and lower mass limits, as determined in this work (at 90% CL).